Interaction Notes 576

Note

November 2002

A NETWORK FORMULATION OF THE POWER BALANCE METHOD FOR HIGH FREQUENCY ELECTROMAGNETIC COUPLING APPLICATIONS

I. Junqua – J.P. Parmantier – F. Issac

DEMR/CDE
ONERA Toulouse
2 avenue Edouard Belin
31055 TOULOUSE
FRANCE

Abstract

This paper deals with the development of the Power Balance approach to estimate high frequency coupling mechanisms in complex systems. Section 2 is devoted to the general principles of this approach as found in the scientific litterature. In section 3, an example of the application and validation of the Power Balance method (under a good shielding approximation) is presented. Then a network formulation of the approach is proposed in section 4. Finally, in section 5 the same example is processed with the network formulation of the Power Balance method by easily adapting the CRIPTE code (dedicated initially to Electromagnetic-Topology).

Intentionally Blank

CONTENTS

Intentionally blank

1. INTRODUCTION

This note deals with the development of the Power Balance method in order to compute high frequency coupling mechanisms in complex systems. Although the coupling of an electromagnetic wave with any system can be theoretically computed thanks to Maxwell's equations, this classic approach may become tedious in the case of high frequency incident electromagnetic environments. Indeed, the use of numerical methods, commonly used (such as FDTD, or MoM) can lead to very large meshes and computationnal ressources which can not be handled by currently available computers. In addition, even if applicable one day, thoses deterministic methods are likely not to cope with the high sensitivity observed in real cases, due to the statistical distribution of internal geometry configurations.

Therefore, for a few years some articles ([1] to [15]) dealing with a method, named Power Balance, are published in the scientific litterature. The objective consists in developing a simple approach which provides an order of magnitude of constraints induced by a high frequency threat on any system. This approach is mainly theoretical and mathematical, and so far, we did not have the chance to find any reference of applications of this method on realistic problems.

2. GENERAL PRINCIPLES OF THE POWER BALANCE METHOD

The Power Balance method qualifies and quantifies from a macroscopic point of view the transfer of energy between cavities and it successively characterizes :

- the penetration of the external incident electromagnetic energy inside the structure
- the electromagnetic environment within the various areas of the structure,
- the coupling of this electromagnetic environment with cables and electronic equipment.

This method is very interesting since it is based on statistical concepts and considers that some parameters (such as the accurate position of an equipment inside a cabin and the exact running of cables,...) are unknown. The main assumption made is that the system under test must be large compared to the wavelength of the electromagnetic threat so that internal electromagnetic environment can be modelled by probabilistic laws.

Figure 1 illustrates how the Power Balance method would solve the problem of RF coupling to an aircraft.

To characterize the response of a system to a high frequency threat, the most important parameters used by the Power Balance method are :

- the incident external power density
- the quality factors and the volumes of the various areas of the system,
- the coupling cross sections of points of entry (POE) such as slots, apertures, windows,..,
- the global running of cable networks
- the quality factors and the volumes of equipment
- the coupling cross sections of equipement POE

(a). Power Density in the test area (S_{inc})

$S_{inc} = \frac{E^2_{RMS,inc}}{\eta}$, $E_{RMs,inc}$: RMS incident electric field

η : Wave impedance in the medium

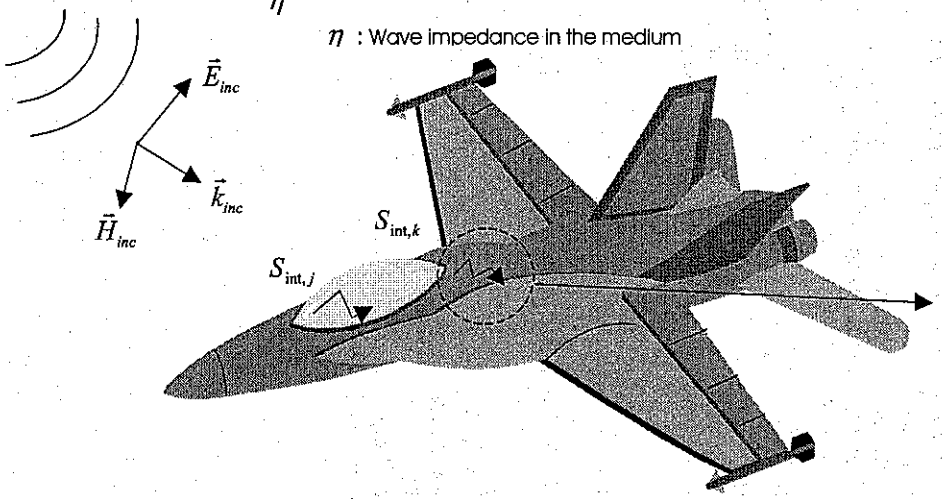

(b). Mean Power Density in cavity j ($S_{int,j}$)

$$S_{\text{int},j} = \frac{\lambda.Q_j}{2\pi.V_j}.(\sum \sigma_n.S_{inc} + \sum \sigma_{j,k}.S_{\text{int},k})$$

σ_n : Coupling cross section of a POE from cavity j towards outside

$\sigma_{j,k}$: Coupling cross section of a POE from cavity j towards cavity k

V_j : Volume of cavity j, Q_j : Quality factor of cavity j

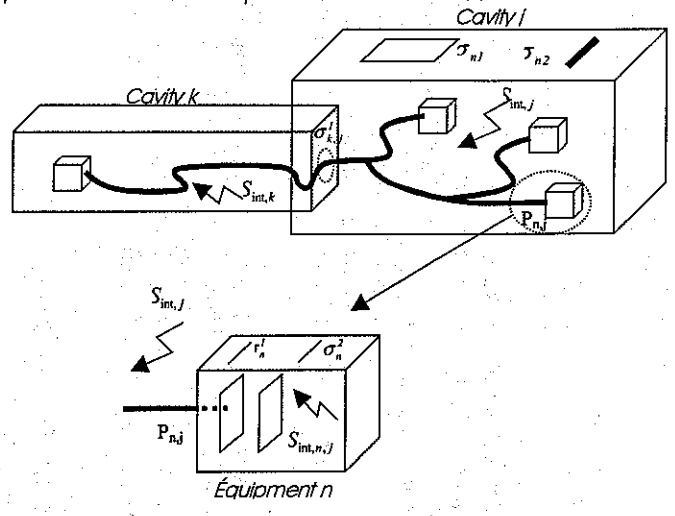

(c). Mean power on cables at the equipment n input of cavity j ($P_{n,j}$)

$$P_{n,j} = \int_z \sigma(z).S_{\text{int}}(z).dz$$

$\sigma(z)$: Coupling cross section of cables connected to equipment I

$S_{\text{int}}(z)$: Mean Power density inside areas in which cables are running

(d). Mean power density in equipment n of cavity j ($S_{int,n,j}$)

$$S_{\text{int},n,j} = \frac{\lambda.Q_n}{2\pi.V_n}.(\sum \sigma_n.S_{\text{int},j} + \sum P_{radiated\_by\_cable\_network})$$

V_n : Volume of equipement n Q_n: Quality factor of equipment n

σ_n: Coupling cross section of POEs of equipment n

Figure 1 : Power Balance method – Successive derivations

2.1 PARAMETERS CHARACTERIZING ELECTROMAGNETIC ENVIRONMENT INSIDE CAVITIES

Let us assume that the dimensions of a cavity are greater than a few wavelengths of the incident electromagnetic interference. We can therefore make the approximation that the cavity behaves as a pseudo-mode stirring chamber. In other words, electromagnetic fields at any point inside the cavity defined by its coordinates (x, y, z) are uniformly distributed random variables of the position. The real and the imaginary parts of these electric fields (and magnetic fields) are gaussian random variables with a mean equal to 0 and with the same variance V_E (and V_H). The mean electromagnetic environment can be considered as pseudo homogeneous and pseudo isotropic. As seen in introduction, high frequency coupling in cavities are charcterized by quality factors and coupling cross sections. In the following paragraphs, we have derived the theoretical expressions of quality factors and coupling cross sections in generic cases.

2.1.1 Quality Factor of a cavity

A quality factor of a cavity is defined as :

$$Q = 2\pi f \frac{W}{P_d} \qquad (1)$$

where f is the frequency, W is the steady state energy available in the cavity and P_d is the dissipated power.

The steady state energy can be expressed as a function of electromagnetic fields inside the cavity :

$$W = \varepsilon \iiint_V \frac{|E|^2}{4} dv + \mu \iiint_V \frac{|H|^2}{4} dv \qquad (2)$$

- V is the cavity volume,
- ε, μ, the permittivity and the permeability of the medium inside the cavity,
- E and H, the peak magnitude of electric and magnetic fields in the cavity at frequency f.

Let us recall that electromagnetic fields inside the cavity are a sum of stationnary waves with a 90 degrees phase shift. Then, at any point inside the cavity, the energy goes alternatly from an inductive form to a capacitive form and the steady state energy, W, can be written as:

$$W = 2\varepsilon \iiint_V \frac{|E|^2}{4} dv = \varepsilon \iiint_V |E_{RMS}|^2 dv \qquad (3)$$

If we assume that the cavity is large compared to the wavelength of the incident electromagnetic interference, electromagnetic fields inside the cavity are random variables. We can write the steady state energy, W, as a function of the variance of the real or imaginary part of the cartesian electric field, V_E :

$$W = 3\varepsilon V.V_E \qquad (4)$$

We can also write the mean power density, S, inside the cavity as (η is the wave impedance of the medium inside the cavity) :

$$S = \frac{3V_E}{\eta} \qquad (5)$$

On the other hand, P_d is the dissipated power inside the cavity and is the sum of various dissipation mechanisms :

- Loss in the cavity walls (P_m),
- Re-Radiation via the Point of entries or generalized apertures (P_{ap})
- Power dissipated in antennas located inside the cavity (P_{ant}),
- Absoption by inner objects in the cavity (P_{obj})

For steady state conditions, we require that the power P_t transmitted inside the cavity is equal to the power dissipated in the four loss mechanisms previously mentioned :

$$P_t = P_d = P_m + P_{ap} + P_{ant} + P_{obj} \quad (6)$$

We can now express the quality factor of the cavity, Q, as a function of elementary quality factor associated to the four loss mechanisms :

$$Q = 2\pi f \frac{W}{P_d} = \frac{1}{\frac{1}{Q_m} + \frac{1}{Q_{ap}} + \frac{1}{Q_{ant}} + \frac{1}{Q_{obj}}}$$

$$Q_m = 2\pi f \frac{W}{P_m} \qquad Q_{ap} = 2\pi f \frac{W}{P_{ap}} \quad (7)$$

$$Q_{ant} = 2\pi f \frac{W}{P_{ant}} \qquad Q_{obj} = 2\pi f \frac{W}{P_{obj}}$$

Considering the structure of this sommation, we can already notice that the quality factors behave as impedances in parallel.

2.1.2 Quality Factor associated to objects absorption

In general, the absorption cross section of a lossy object depends on the incidence angles and polarisation of the incident interference and is defined by the transfer function between the dissipated power by the object and the incident power density on this object :

$$P_{obj} = \sigma_{obj}(\theta, \varphi, \psi).S(\theta, \varphi, \psi) \quad (8)$$

If we assume that the cavity containing the object is large compared to the incident electromagnetic interference, it behaves as a pseudo-mode stirring chamber. Therefore, the object is bathed in an infinity of plane waves with random incidences and polarisations. We can write the following mean dissipated power :

$$P_{obj} = \frac{1}{4\pi}\int_{\Omega} \sigma_{obj}(\Omega).S(\Omega).d\Omega$$

$$P_{obj} = \langle \sigma_{obj} \rangle . \frac{3V_E}{\eta} \quad (9)$$

- $\langle \sigma_{obj} \rangle$ is the averaged absorption cross section of the object
- $3.V_E/\eta$ is the average power density in the cavity (see equation 5)

The result for the quality factor, Q_{obj}, associated to absoption by lossy objects is :

$$Q_{obj} = \frac{2\pi V}{\lambda \langle \sigma_{obj} \rangle} \quad (10)$$

2.1.3 Particular case of wall losses

We can find in the litterature [1] different theoretical developments to quantify the power dissipated in cavity walls, where the cavity is considered as a mode stirring chamber. In either case the result for the quality factor Q_m and the average cross section $\langle \sigma_m \rangle$ are :

$$Q_m = \frac{3V}{2S} \cdot \frac{\pi f \mu_0}{R_s} = \frac{3V}{2S} \cdot \sqrt{\frac{\pi f \mu_0 \sigma}{\mu_r}}$$

$$\langle \sigma_m \rangle = \frac{4S.R_s}{3c.\mu_0} = \frac{4\pi S}{3\lambda} \cdot \sqrt{\frac{\pi f \mu_0 \sigma}{\mu_r}} \quad (11)$$

- S is the cavity surface area,
- V is the volume of the cavity,
- μ_r is the relative wall permeability,
- σ is the wall conductivity,
- R_s is the wall surface impedance

2.1.4 Particular case of re-radiation through POE

An aperture, or more generally a POE, is characterized by its transmission coupling cross section, σ_{ap}, defined as the transfer function between the power transmitted from area 1 to area 2 (P_{t2}) and the power density in area 1 (S_1) (see figure 2).

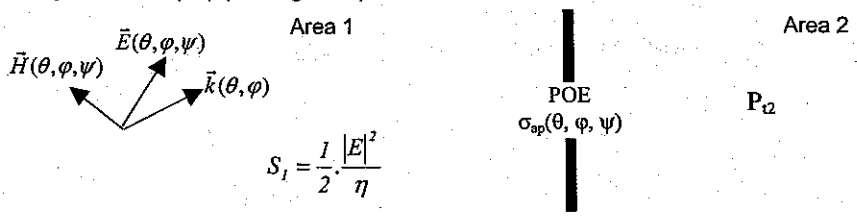

Figure 2 : Transmission coupling cross section of a POE

$$P_{t2} = \sigma_{ap}(\theta,\varphi,\psi).S_1 \qquad (12)$$

If we now assume that both cavities behave as pseudo mode stirring chambers, we can write :

$$P_{ap} = \frac{1}{2}.\frac{1}{4\pi}.\int_{\Omega} P_{t2}(\Omega).d\Omega = \frac{3V_E}{\eta}.\langle\sigma_{ap}\rangle \qquad (13)$$

- the factor ½ is introduced in order to take into account only waves propagating from area 1 to area 2.
- $<\sigma_{ap}>$ is the averaged transmission coupling cross section,
- V_E is the variance of the real or imaginary part of a cartesian electric field in Area 1.

Therefore, introducing (4) and (9) in (7), the result for the quality factor associated to re-radiation via apertures is :

$$Q_{ap} = \frac{2\pi V}{\lambda\langle\sigma_{ap}\rangle} \qquad (14)$$

In the litterature [1] to [4], we can find some expressions of the coupling cross sections that we will list later on.

2.1.5 Particular case of losses in antennas

Let us consider the equivalent electric scheme (figure 3) of a receiving antenna where :

- R is the input impedance of the receiver connecting to the receiving antenna,
- R_r, the radiation resistance of the antenna,
- X_r, the reactive impedance of the antenna,
- V_0, the voltage generator representing the coupling with the electromagnetic field,
- V, the voltage induced at the receiver input,

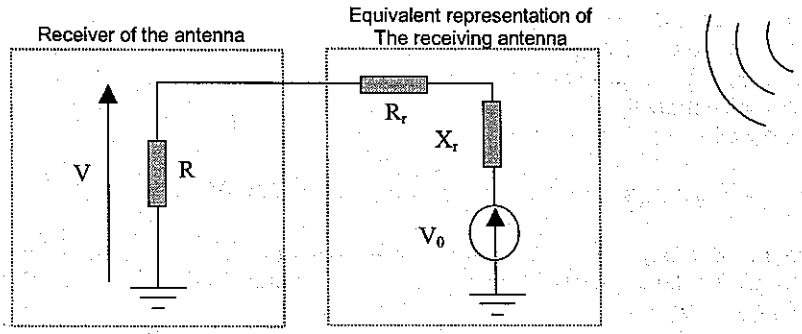

Figure 3 : Equivalent scheme of a receiving antenna

The power dissipated in the resistance R is :

$$P = \frac{|V|^2}{2.R} = \left(1 - |S_{11}|^2\right).\frac{|V_0|^2}{8.R_r}$$
$$S_{11} = \frac{R_r + j.X_r - R}{R_r + j.X_r + R} \qquad (15)$$

- S11 is the reflection coefficient of the antenna (referenced to the impedance of the receiver of the antenna) identical in reception and transmission (when the antenna is only made of reciprocial media).
- $\left(1 - |S_{11}|^2\right)$ is the mismatch factor of the antenna.

If we assume that the antenna sees an incident plane wave with an incidence (θ, φ) and a polarisation ψ, then we can express V_0 as a function of the receiving effective height of the antenna :

$$V_0 = h(\theta,\varphi,\psi).E_{RMS}(\theta,\varphi,\psi)$$
$$|h(\theta,\varphi,\psi)|^2 = \frac{\lambda^2}{120\pi}.R_r.G(\theta,\varphi,\psi) \qquad (16)$$

- $h(\theta,\varphi,\psi)$ is the effective height in the receiving direction (θ,φ,ψ),
- $E_{RMS}(\theta,\varphi,\psi)$ is the RMS incident electric field in the direction (θ,φ,ψ),
- $G(\theta,\varphi,\psi)$, the antenna gain in the receiving direction (θ,φ,ψ),

We can re-write the power dissipated at the antenna output when the antenna is illuminated by a plane wave :

$$P = \frac{\lambda^2}{8\pi}.\frac{\left(1 - |S_{11}|^2\right)}{120\pi}.G(\theta,\varphi,\psi).|E_{RMS}(\theta,\varphi,\psi)|^2 \qquad (17)$$

If we now assume that the antenna is located in a pseudo-mode stirring chamber (such as in a cavity large compared to the wavelength), the antenna will receive plane waves from any direction and polarisation. Therefore, the mean power dissipated at the antenna output is computed as:

$$P_{ant} = \frac{\lambda^2}{8\pi}.\frac{\left(1 - |S_{11}|^2\right)}{\eta}.\int_{\Omega}\frac{G(\Omega).|E_{RMS}(\Omega)|^2}{4\pi}.d\Omega$$
$$P_{ant} = \frac{\lambda^2}{8\pi}.\left(1 - |S_{11}|^2\right)\frac{3.V_E}{\eta} \qquad (18)$$

Finally, the quality factor associated to the loss in receiving antennas and it coupling cross section are given by :

$$Q_{ant} = 2\pi f.\frac{W}{P_{ant}} = \frac{16.\pi^2.V}{\lambda^3.\left(1-\left|S_{11}\right|^2\right)}$$
$$\left\langle \sigma_{ant} \right\rangle = \frac{\lambda^2}{8\pi}.\left(1-\left|S_{11}\right|^2\right) \qquad (19)$$

2.2 TRANSMISSION CROSS SECTION OF APERTURE-TYPE POES

In this section, 'aperure' is a general word that includes slots, seams, windows,... Aperture theory has been developed for apertures in flat, perfectly conducting screens of infinite extent and zero thickness. Then, we will assume that the shield is locally planar and that the thickness of the shield is small. Aperture theory can be subdivided into three cases where the aperture dimensions are either small, comparable or large compared to the wavelength.

i) For electrically large apertures, the geometrical optics approximation yields to :

$$\sigma_{ap}(\theta) = A\cos(\theta) \qquad (20)$$

- A is the aperture area
- θ is the incident elevation angle, that is to say the angle between the propagation vector and the normal vector to the aperture.

If this aperture is now illuminated by a sum of plane waves of random incidence, we obtain the following average cross section :

$$\left\langle \sigma_{ap} \right\rangle = \frac{1}{2\pi}.\int_0^{2\pi} d\varphi.\int_0^{\pi/2} A\cos(\theta)\sin(\theta)d\theta = \frac{A}{2} \qquad (21)$$

ii) For electrically small apertures, polarizability theory states that the transmitted fields are those of induced electric and magnetic dipoles moments. This theory yields a transmission cross section that is proportionnal to frequency to the fourth power.

$$\sigma_{ap} = C.\left(\frac{2\pi f}{c}\right)^4 \qquad (22)$$

where C depends on incident angle, polarization and aperture size and shape, but is independent of frequency. We can find in the litterature [1] to [4] the expression of C and of the average coupling cross section for specific geometry of apertures. For example, the average coupling cross section of a circular aperture of radius a is given by :

$$\left\langle \sigma_{ap} \right\rangle = \frac{16}{9\pi}.\left(\frac{2\pi}{\lambda}\right)^4.a^6 \quad for \quad f \le \frac{1,3c}{2\pi a} \qquad (23)$$

iii) In the resonance region, the aperture dimensions are comparable to the wavelength, and the frequency dependance of σ_{ap} depends on the aperture shape. Numerical methods or measurements are generally required to determine σ_{ap} and the average coupling cross section $\langle\sigma_{ap}\rangle$ for such cases.

3. ANALYTICAL EXAMPLE OF AN APPLICATION OF THE POWER BALANCE METHOD

3.1 SYSTEM UNDER TEST

Let us consider a cylindrical system constituted of two cavities [16] (see figure 4). The lower cavity is made of aluminium and the upper cavity is partially composite. On the plate separating both cavities, there is a small circular hole and there is also a square aperture on the upper cavity.

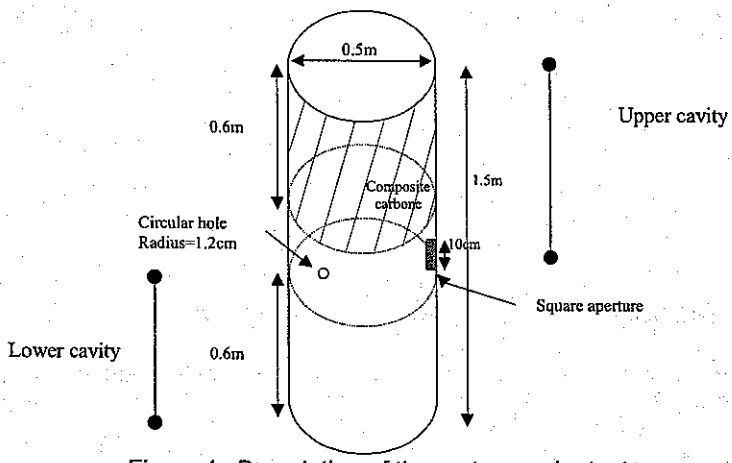

Figure 4 : Description of the system under test

The goal of this study is to estimate, thanks to the Power Balance approach, the electromagnetic environment in the lower volume, when a transmitting antenna is located in the upper volume. To do this, we insert in both cavities a waveguide, a transmitting one in the upper volume and a receiving one in the lower volume. The experimental configuration consists in measuring the transfer function $[S_{21}]$ between these two waveguides. In order to consider the system as 2 mode stirring cavities, we also install a mechanical stirrer in the upper volume (see figure 5). Therefore the $[S_{21}]$ parameter is measured at each stirrer position. We finally process these measurements to extract the average and the variance of $[S_{21}]$ over a complete rotation of the stirrer and compare the measured variance with the estimated one by the Power Balance simulation.

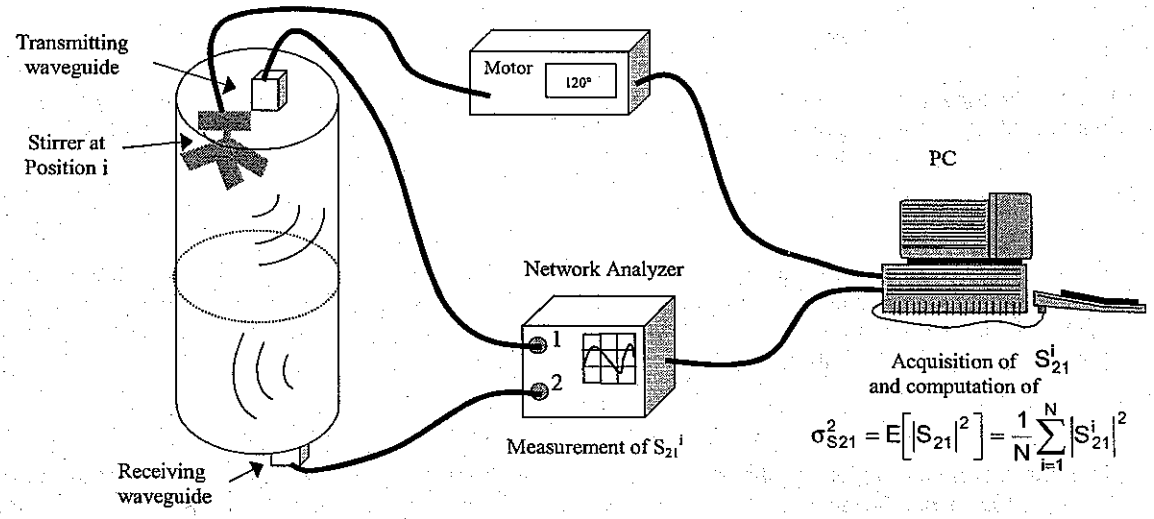

Figure 5 : Experimental configuration

3.2 APPLICATION OF THE POWER BALANCE METHOD

By definition, the variance of S_{21}, σ^2_{S21}, is the transfer function between the average power dissipated in the receiving waveguide, P_{ant}, and the incident power at the transmitting waveguide input, P_{inc}:

$$\sigma^2_{S21} = \frac{P_{ant}}{P_{inc}} \qquad (24)$$

Let us call :

- P_t, the total power transmitted by the waveguide located in the upper cavity,
- S_{11}, the reflection coefficient of the transmitting waveguide
- S_{22}, the reflection coefficient of the receiving waveguide.
- S_u, the average power density in the upper volume,
- S_l, the average power density in the lower volume.

From equations (24) and (15), we can write :

$$P_t = \left(1-|S_{11}|\right)^2 .P_{inc} \quad and \quad P_{ant} = \frac{\lambda^2}{8\pi}\left(1-|S_{22}|^2\right)S_l$$
$$\sigma^2_{S21} = \frac{P_{ant}}{P_{inc}} = \frac{\left(1-|S_{11}|^2\right)\left(1-|S_{22}|^2\right)\lambda^2 .S_l}{8.\pi .P_t} \qquad (25)$$

We can re-write the expression of a cavity quality factor as follows (from equations (1), (4) and (5)):

$$Q = 2\pi f \frac{W}{P_d} = 2\pi f \frac{W}{P_t} = \frac{2\pi}{\lambda}.\frac{V.S}{P_t} \qquad (26)$$

- P_t is the total power transmitted in the cavity
- V is the cavity volume,
- S is the average power density in the cavity

If we apply equation (26) to our problem and if we assume that there is no retro-action of the lower cavity on the upper cavity (in other words, we apply the good shielding approximation [18]), we obtain :

$$S_u = \frac{\lambda.Q_u}{2\pi V_u}.P_t \quad and \quad S_l = \frac{\lambda.Q_l}{2\pi V_l}.\frac{\langle\sigma_h\rangle}{2}.S_u \qquad (27)$$

- Q_u is the upper cavity quality factor
- V_u is the upper cavity volume
- Q_l is the lower cavity quality factor
- V_l is the lower cavity volume
- S_l is the average power density in the lower volume
- $\langle\sigma_h\rangle$ is the average coupling cross section of the circular hole located on the transition plate

The quality factors of both cavities, Q_u and Q_l are derived from equations (7) to (19):

$$\frac{1}{Q_u} = \frac{1}{Q^u_{wall}} + \frac{1}{Q_{ap}} + \frac{1}{Q^1_{ant}} + \frac{1}{Q^u_h}$$
$$\frac{1}{Q_l} = \frac{1}{Q^l_{wall}} + \frac{1}{Q^2_{ant}} + \frac{1}{Q^l_h} \qquad (28)$$

where :

- Q^u_{walls} represents walls loss in the upper volume,
- Q_{ap}, re-radiation through the square aperture of the upper volume,
- Q^1_{ant}, loss in the transmitting antenna,
- Q^u_h, re-radiation through the circular hole in the upper volume,
- Q^l_{walls}, walls loss in the lower volume,
- Q^2_{ant}, loss in the receiving antenna,
- Q^l_h, re-radiation through the circular hole in the lower volume

By applying equations (21) and (23) to the circular hole and to the square aperture, we obtain:

- coupling cross section of the circular hole (of radius a), $\langle\sigma_h\rangle$:

Low frequency formulation $$\langle \sigma_h \rangle = \frac{16}{9\pi}\left(\frac{2\pi}{\lambda}\right)^4 .a^6 \quad f \le \frac{1.3c}{2\pi a}$$

High frequency formulation $$\langle \sigma_h \rangle = \frac{\pi a^2}{2} \quad f \ge \frac{1.3c}{2\pi a}$$ (29)

- coupling cross section, $<\sigma_{ouv}>$, of the square aperture (area of the aperture = dxd)

High frequency formulation $$\langle \sigma_{ouv} \rangle = \frac{d^2}{2}$$ (30)

For our numerical application, we will consider the following data :

- Conductivity of the composite carbon=$3.10^4 S.m^{-1}$
- Conductivity of the aluminium=$10^7 S.m^{-1}$

In figure 6, we represent versus frequency :

- the global and elementary quality factors of the upper volume (composite volume),
- the global and elementary quality factors of the lower volume (metallic volume).

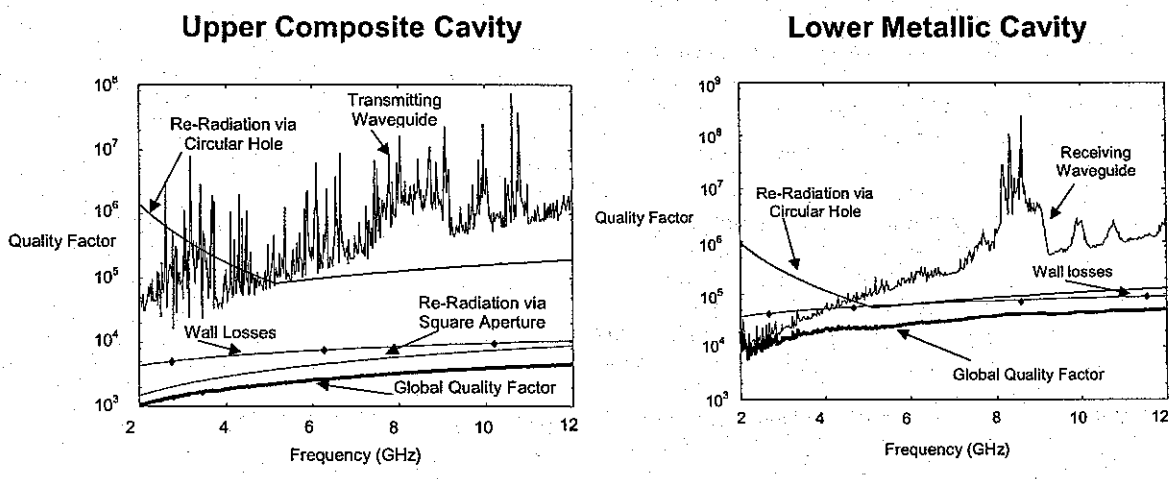

Figure 6 : Quality factor of Upper and Lower Cavities

In figure 7, we represent versus frequency :

- the measured variance of S_{21},
- the computed variance S_{21} (equations (25) and (27)).
- the global and elementary quality factors of the lower volume (metallic volume).

Measured and computed results show quite a good agreement in the whole frequency range. The best agreement is obtained at high frequency (above 9GHz). In low frequency (between 2GHz and 4GHz), we can note some discrepancies. They can be explained by the fact that in that frequency range, the system may not be considered as a pseudo-mode stirring chamber (as we assume in our theoretical development) and by the fact that we introduce crude analytical formulas. Let us assume that the frequency waveform observed on the plots comes from the measurements of S_{11} and S_{22} waveguides which are the only measured parameters introduced in the Power Balance computation.

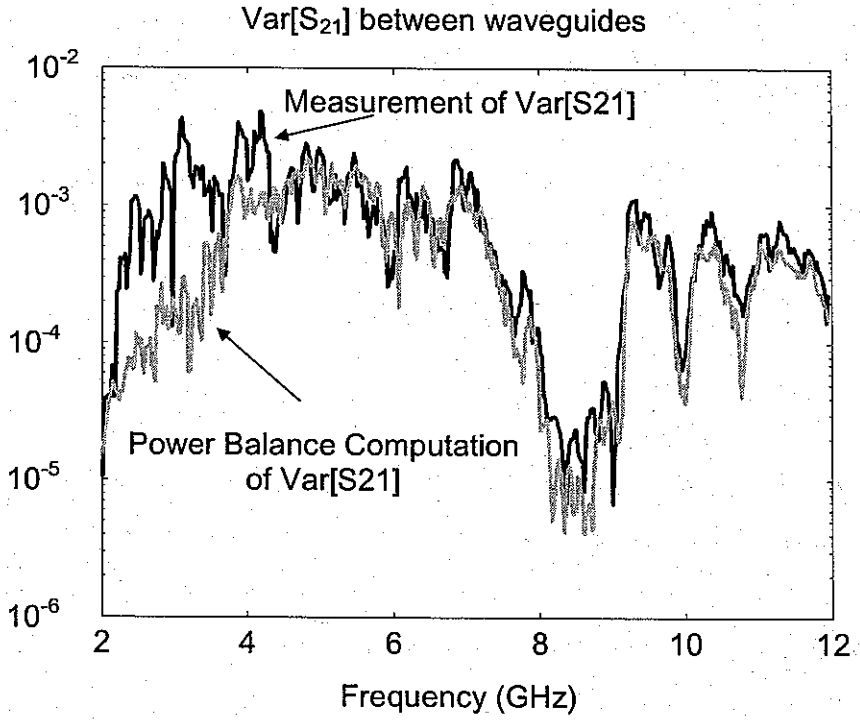

Figure 7 : Application of the Power Balance method to the cylindrical 2-cavities system – Measurement and computation of Var[S_{21}]

4. TOWARDS A NETWORK FORMULATION OF THE POWER BALANCE METHOD

4.1 INTRODUCTION

The previous theoretical developments show that a network formulation could be applied to the Power Balance method. We already said that the summation rule of the quality factors is similar to the summation rule of impedances in parallel (see equation (7)). Equation (9) provides a linear relation between the two main unknowns of the problem :

- the dissipated power, P, and
- the power density, S.

The linear factor is made by the mean of the coupling cross section <σ>. <σ> being proportional to the inverse of Q (see equation (10)), we can make it analogous to an admittance. Therefore, the dissipated power, P, becomes analogous to a current and the power density, S, to a voltage. The different analogy are summarized here after :

$$\begin{aligned} \text{Dissipated Power } P &\equiv \text{Current } I \\ \text{Power Density } S &\equiv \text{Voltage } V \\ \text{Coupling Cross Section } \sigma &\equiv \text{Admittance } Y \\ P = \sigma.S &\equiv I = Y.V \end{aligned} \qquad (31)$$

We can see that the quality factor Q is not directly used in the linear equation relating P and S ; however it is a measurable quantity allowing one to derive the value of the coupling cross section <σ> by :

$$\langle \sigma \rangle = \frac{2\pi V}{\lambda Q} \qquad (32)$$

Besides the organization of the calculations may be based on an interaction diagram sequence as done in electromagnetic topology, which follows the running of the power transferred into the cavities. If we consider our previous example, we can draw the following interaction graph (Figure 8).

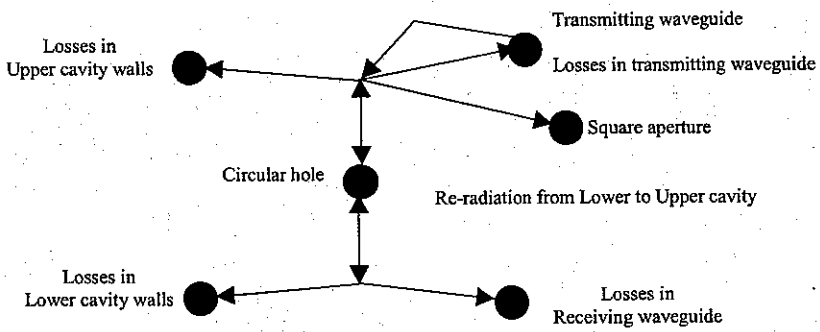

Figure 8 : Interaction graph of the cylindrical structure excited by the waveguide in the upper cavity

At each node, we associate a coupling cross section linking the power dissipated in the component and the power density. Each branch represents the propagation of the power through cavities and between different nodes. The unknown of the interaction graph are the dissipated power and the power density at each node. Note the bi-directed arrows at the level of the circular hole junction related to the possible retro-action of the Lower cavity to the Upper cavity through the hole.

4.2 Analogy to the transmission line theory – Network formulation

4.2.1 Network Formulation

Let us consider the simpler case of a single enclosure (with walls of finite conductivity) containing a transmitting antenna. The only losses to take into account are the losses in the walls and in the antenna. The corresponding interaction graph is therefore as illustrated in figure 9.

Let
- P^1, be the mean power dissipated in the walls,
- P^2, the mean power dissipated in the mismatched transmitting antenna,
- P_{inc}, the power delivered by the transmitting antenna,
- S, the power density in the cavity,
- σ_1^{-1}, the inverse of the coupling cross section of the walls,
- σ_2^{-1}, the inverse of the coupling cross section of the transmitting antenna.

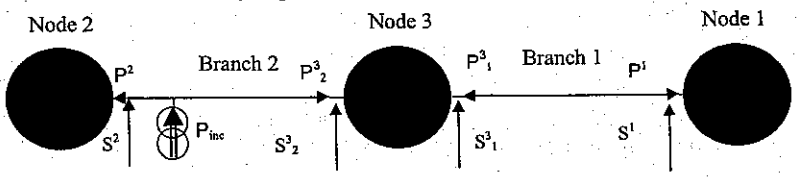

Figure 9 : Case of a cavity with finite conductivity walls and a transmitting antenna

The different equations linking the unknows are :

$$Node\ 1: \begin{bmatrix} 1 & -\sigma_1^{-1} \end{bmatrix} \begin{bmatrix} S^1 \\ P^1 \end{bmatrix} = [0] \qquad Node\ 2: \begin{bmatrix} 1 & -\sigma_2^{-1} \end{bmatrix} \begin{bmatrix} S^2 \\ P^2 \end{bmatrix} = [0]$$

$$Node\ 3: \begin{bmatrix} 1 & 0 & -1 & 0 \\ 0 & 1 & 0 & 1 \end{bmatrix} \begin{bmatrix} S_1^3 \\ P_1^3 \\ S_2^3 \\ P_2^3 \end{bmatrix} = \begin{bmatrix} 0 \\ 0 \end{bmatrix} \tag{33}$$

$$Branch\ 1: \begin{bmatrix} 1 & 0 & -1 & 0 \\ 0 & 1 & 0 & 1 \end{bmatrix} \begin{bmatrix} S_1^3 \\ P_1^3 \\ S^1 \\ P^1 \end{bmatrix} = \begin{bmatrix} 0 \\ 0 \end{bmatrix} \qquad Branch\ 2: \begin{bmatrix} 1 & 0 & -1 & 0 \\ 0 & 1 & 0 & 1 \end{bmatrix} \begin{bmatrix} S_2^3 \\ P_2^3 \\ S^2 \\ P^2 \end{bmatrix} = \begin{bmatrix} 0 \\ P_{inc} \end{bmatrix}$$

The resulting matrix system to solve is :

$$\begin{bmatrix} 1 & -\sigma_1^{-1} & 0 & 0 & 0 & 0 & 0 & 0 \\ -1 & 0 & 1 & 0 & 0 & 0 & 0 & 0 \\ 0 & 1 & 0 & 1 & 0 & 0 & 0 & 0 \\ 0 & 0 & 1 & 0 & -1 & 0 & 0 & 0 \\ 0 & 0 & 0 & 1 & 0 & 1 & 0 & 0 \\ 0 & 0 & 0 & 0 & 1 & 0 & -1 & 0 \\ 0 & 0 & 0 & 0 & 0 & 1 & 0 & 1 \\ 0 & 0 & 0 & 0 & 0 & 0 & 1 & -\sigma_2^{-1} \end{bmatrix} \begin{bmatrix} S^1 \\ P^1 \\ S_1^3 \\ P_1^3 \\ S_2^3 \\ P_2^3 \\ S^2 \\ P^2 \end{bmatrix} = \begin{bmatrix} 0 \\ 0 \\ 0 \\ 0 \\ 0 \\ 0 \\ P_{inc} \\ 0 \end{bmatrix} \tag{34}$$

The expected solution of this system is consistent with the Power Balance approach since we can easily relate the coupling cross sections to quality factors. As said before, quality factors are only intermediate parameters which can be easily measured to then estimate coupling cross sections. The power density S ($S=S^2=S^1=S^3_2=S^3_1$) is:

$$S = \frac{P_{inc}}{\sigma_1 + \sigma_2}$$

$$\sigma_1 = \frac{2\pi V}{\lambda . Q_1} \ and \ \ \sigma_2 = \frac{2\pi V}{\lambda . Q_2} \tag{35}$$

$$S = \frac{\lambda}{2\pi V} \cdot \frac{P_{inc}}{\frac{1}{Q_1} + \frac{1}{Q_2}} = \frac{\lambda . Q . P_{inc}}{2\pi V}$$

where V is the volume of the cavity, Q_1 and Q_2 respectively the quality factor associated to losses in the walls and in the transmitting antenna and Q the total quality factor of the cavity. We are able to derive a network equation relating all the unknowns of the network [17]. The BLT formulation of this network equation presents the advantage of being totally dedicated to an Electromagnetic Topology approach.

4.2.2 Wave definition

As we can see, we can easily make an analogy with the circuit approach where, the dissipated power is homogeneous to a current, the power density to a voltage and the coupling cross section to an admittance. Therefore, at each branch number i, connecting two nodes n and m, we introduce 2 waves, combining equivalent powers, illustrated in figure 10, where A_c is a reference characteristic coupling cross section (homogeneous to an admittance) to be defined latter on in this document:

$$W_i^n(0) = A_c.S_i^n - P_i^n \qquad W_i^n(l) = A_c.S_i^m + P_i^m$$
$$W_i^m(0) = A_c.S_i^m - P_i^m \qquad W_i^m(l) = A_c.S_i^n + P_i^n \tag{36}$$

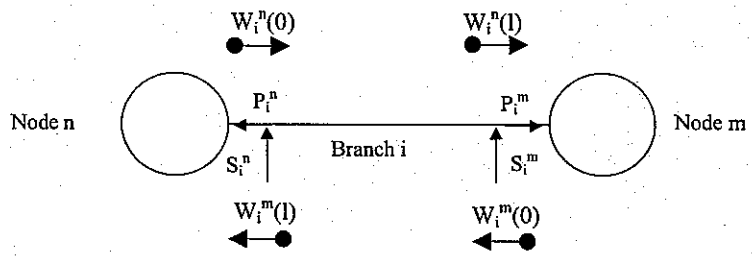

Figure 10 : Definition of waves on each branch i connecting 2 nodes n and m

Note that, with reference to the usual form of the BLT equation, the $W_i^n(z)$ waves are equivalent to equivalent combined power (or analogous to combined equivalent currents).

4.2.3 Propagation equation

In the power balance approach, there is no notion of propagation as in the transmission line theory and as in electromagnetic topology (BLT1 form). We can write :

$$S_i^n = S_i^m \qquad P_i^n = -P_i^m$$
$$W_i^n(l) = W_i^n(0) \quad or \quad [1]\left[W_i^n(0)\right] = \left[W_i^n(l)\right] \tag{37}$$
$$W_i^m(l) = W_i^m(0) \quad or \quad [1]\left[W_i^m(0)\right] = \left[W_i^m(l)\right]$$

In that case, the propagation matrix on a branch, commonly named $[\Gamma^i]$ in the electromagnetic topology (or BLT1 equation) [18], is reduced to the identity matrix, [1]. This approach is equivalent to shrink all the tube lengths to zero and leads to a BLT2 type network equation.

If we apply a source on the branch, such as an incident power generator P_{inc} (homogeneous to a current generator) or/and an incident power density generator S_{inc} (homogeneous to a voltage generator)(see figure 11), the propagation equation on the branch becomes:

$$\left[W_i^n(l)\right] = [1]\left[W_i^n(0)\right] + \left[W_s^n\right] \qquad \left[W_s^n\right] = A_c.[S_{inc}] + [P_{inc}]$$
$$\left[W_i^m(l)\right] = [1]\left[W_i^m(0)\right] + \left[W_s^m\right] \qquad \left[W_s^n\right] = A_c.[-S_{inc}] + [P_{inc}] \tag{38}$$

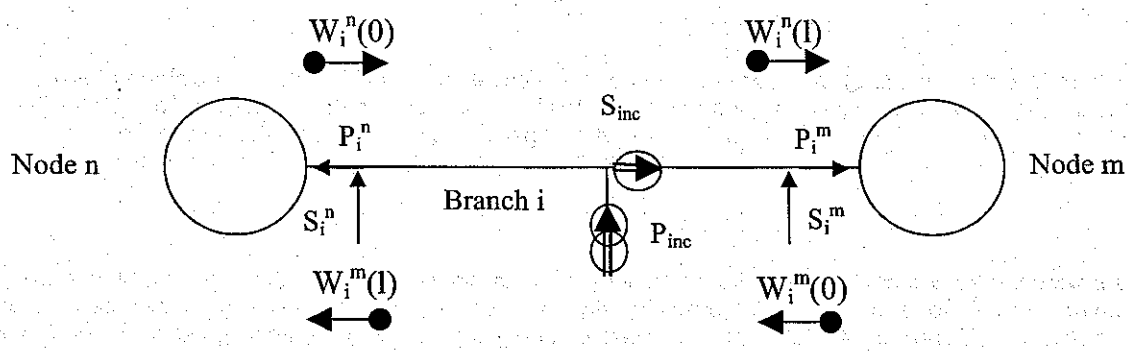

Figure 11 : Sources applied on a branch

Note the analogy of S_{inc} and P_{inc} with voltage and current generator symbols.

4.2.4 Scattering at nodes

Let us now consider 2 branches i and j, connecting respectively a node n to a node m and a node p (figure 12):

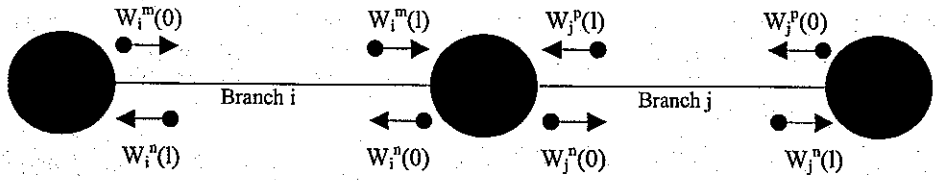

Figure 12 : Definition of waves at nodes

Let us remember that in the Power Balance approach a node represents any dissipation of power in cavities. Each node is therefore characterized by a coupling cross section analogous to an admittance. At each node there is nothing preventing us from introducing a scattering matrix linking waves at the input and at the output of nodes. Let $[\Sigma^n]$, be the scattering matrix (deduced from the coupling cross section and referenced to a coupling cross section A_c which is identical to the previous characteristic coupling cross section introduced in the propagation equation) :

$$\begin{bmatrix} W_i^n(0) \\ W_j^n(0) \end{bmatrix} = [\Sigma^n] \begin{bmatrix} W_j^m(l) \\ W_j^p(l) \end{bmatrix} \tag{39}$$

4.2.5 Generalization of the BLT equation on a multiple-branch network

If we now gather :

- the waves $[W_i^n(0)]$ and $[W_i^n(l)]$ of a global network in super-vectors [W(0)] and [W(l)],
- the sources on each branch in a super vector $[W_s]$,
- the propagation matrices $[\Gamma_i]$ (equal to the identity) of branches in a super matrix $[\Gamma]$,
- the scattering matrices $[\Sigma^n]$ of nodes in a super matrix $[\Sigma]$,

we obtain the well known BLT equation [17,18] which enables to compute any travelling wave in our network.

$$\begin{aligned} &\text{Propagation Equation :} && [W(l)] = [\Gamma][W(0)] + [W_s] \\ &\text{Scattering Equation :} && [\mathrm{W}(0)] = [\Sigma][W(l)] \\ &\text{BLT Equation :} && (I - [\Sigma][\Gamma])[\mathrm{W}(0)] = [\Sigma][W_s] \end{aligned} \tag{40}$$

Finally, by combining these waves, we obtain any dissipated power, P, and power density, S, in our network (in other terms in cavities) (see equation (36)):

$$\begin{aligned} [P] &= \frac{1}{2}.([W(l)] - [W(0)]) \\ [\mathrm{S}] &= \frac{1}{2.A_c}.([W(l)] + [W(0)]) \end{aligned} \tag{41}$$

4.2.6 Characteristic coupling cross section, A_c

As we mentionned before, in the network formulation of the Power Balance approach, we need to introduce a characteristic coupling cross section, A_c, which is homogeneous to an admittance. To be consistent with our theoretical development, we can choose it to be the coupling cross section of a matched receiving antenna:

$$A_c = \frac{\lambda^2}{8.\pi} \tag{42}$$

5. NUMERICAL APPLICATION OF THE NETWORK FORMULATION OF POWER BALANCE APPROACH

5.1 INTRODUCTION

For this numerical application, we considered the same test case as in paragraph 3 . The aim is now to compute with the network formulation the mean power dissipated at the receiving waveguide located in the lower volume of the cylindrical mock-up (figures 4 and 5) and to compare the computed dissipated powers to the measured one (σ^2_{S21}).

Any network oriented computer code may be used to solve the network method presented in this document. However, with the idea of extending this approach with Electromagnetic-Topology concepts, a code solving the BLT equation is more appropriate. This is the reason why we have chosen the CRIPTE code in our application. The CRIPTE code, initially devoted to compute coupling mechanisms on transmission lines, has been developed and validated at ONERA for about 10 years ([19]).

5.2 NETWORK REPRESENTATION OF THE TEST CASE

In the CRIPTE code, each junction (or node) may be described by [S], [Y], or [Z] parameters. So we choose to characterize each junction of our problem by an admittance ([Y] parameters) equal to the coupling cross section of the loss component of the problem. Since there is no propagation on tubes, they are defined as zero-length tubes. The source (power transmitted by the antenna) is applied as an equivalent current generator on a zero-length tube. The electrical circuit corresponding to our test case is as follows (Figure 13), where AG represent the various coupling cross sections :

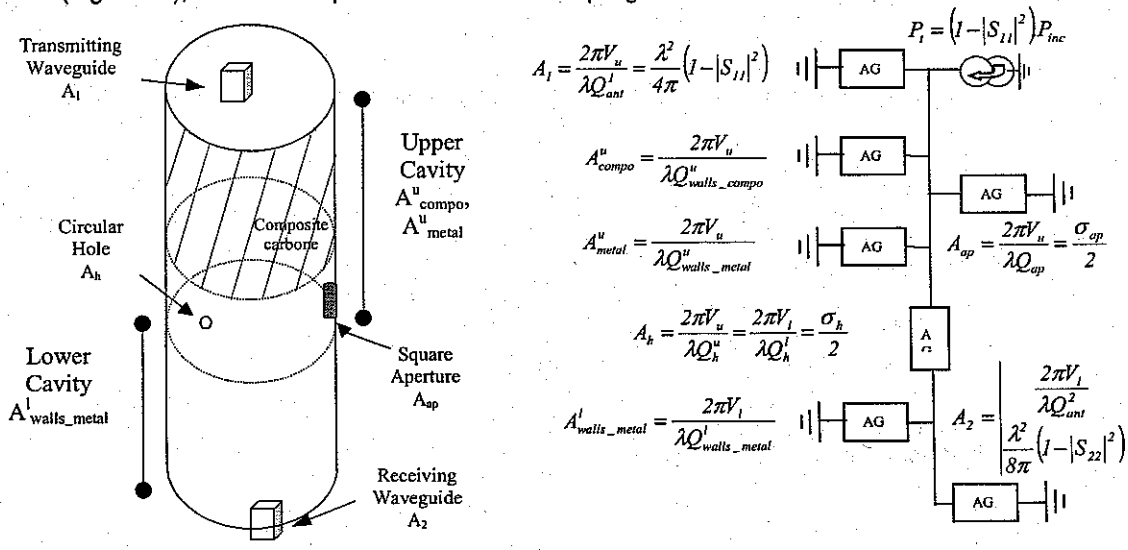

Figure 13 : Electrical circuit representing the test case

- A_1 is the coupling cross section of the transmitting antenna,
- A^u_{compo} is the coupling cross section representing losses in composite walls of the upper volume,
- A^u_{metal} is the coupling cross section representing losses in metallic walls of the upper volume,
- A_{ap}, is the equivalent coupling cros section of the square aperure located in the upper volume,
- A_h is the equivalent coupling cross section of the circular hole on the intermediate plate connecting both cavities,
- $A^l_{walls\_metal}$ is the coupling cross section representing losses in metallic walls of the lower volume,
- A_2 is the coupling cross section of the receiving antenna.

The CRIPTE – code network modelling the electromagnetic problem is drawn in figure 14, where (see equations (24) to (30)):

- Junction 1(AEf.s) represents the dissipation of energy in the transmitting waveguide by a coupling cross section A_1,
- Junction 3 (Mur_compo.s) represents the dissipation of energy in the composite walls of the upper volume by a coupling cross section A_{compo}^{u},
- Junction 4 (Mur_metal.s) represents the dissipation of energy in the metallic walls of the upper volume by A_{metal}^{u},
- Junction 5 (TRAPPE.s) represents the re-radiating power through the square aperture by the coupling cross section A_{ouv},
- Junction 2 (VC_ideale.s) represents the upper ideal cavity,
- Junction 6 (TROU.s) represents the circular aperture between both cavity by A_h,
- Junction 7 (VM_ideale.s) represents the lower ideal cavity,
- Junction 8 (ARf.s) represents the dissipation of energy in the receiving waveguide by A_2,
- Junction 9 (Mur_metal_metal.s) represents the dissipation of energy in the metallic walls of the lower volume by A_{metal}^{l},
- All the branches have a null length in order to represent the fact that the propagation matrix is the identity matrix,
- On tube 1, we apply an incident power generator equal to the incident power transmitted by the transmitting waveguide in the upper volume, P_t.

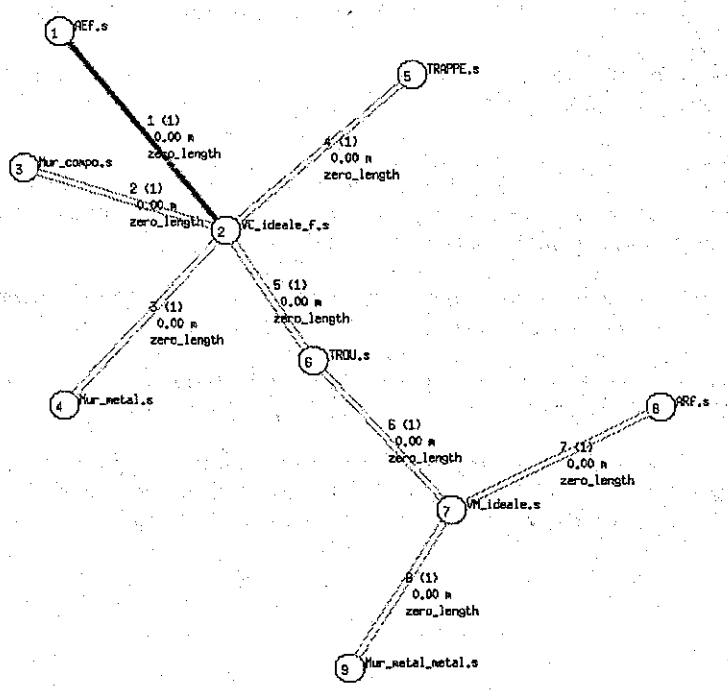

Figure 14 : Network representation of the test case

By solving analytically the electrical circuit, we obtain the following power densities in the upper and lower volume (S_u, S_l) and the following dissipated power by the receiving waveguide, P_{ant} :

$$S_u = \frac{\lambda . P_t}{2\pi . V_u . \left(\frac{1}{Q^1_{ant}} + \frac{1}{Q_{ouv}} + \frac{1}{Q^u_{compo}} + \frac{1}{Q^u_{metal}} + \frac{1}{Q^u_h + \left(\frac{1}{Q^1_{metal}} + \frac{1}{Q^2_{ant}} \right)^{-1}} \right)}$$

$$S_l = \frac{\lambda}{2\pi . V_l} . Q_l . \frac{\sigma_h}{2} . S_u \qquad (43)$$

$$P_{ant} = \frac{\lambda^2}{8\pi} . \left(1 - |S_{22}|^2\right) S_l$$

We see that the resolution of this electrical circuit gives a power density in the upper volume which is slightly different from the one we obtained previously (see equations (26) and (27)). Indeed when we applied the power balance approach with the good shielding approximation (paragraph 3), we did not consider the fact that the upper volume was loaded by the lower one. In other words, we neglected the retro-action term $\left(\frac{1}{Q^1_{metal}} + \frac{1}{Q^2_{ant}} \right)^{-1}$ beyond Q^u_h. Therefore, we expect that the network formulation of the power balance approach will give more accurate results than in figure 7 since it takes into account the whole retroaction between different cavities.

In figure 15, we have drawn versus frequency:

- the measured variance of S_{21}, which is the mean power dissipated by the receiving waveguide
- the computed mean power dissipated by the receiving waveguide thanks to the network formulation of the power balance approach (CRIPTE code)

Indeed, we observe a very good agreement in the whole frequency range between measurement and computation of the dissipated power at the receiving waveguide. We must not forget that we introduced analytical formula usually available for generic geometries:

- to model radiation through the square aperture and through the circular hole ,
- to model the losses via the walls of the mock-up.

Remember also that the only measurements we had to take into account in our computation were the reflection parameters (S_{11} and S_{22}) in free space of the transmitting and receiving waveguides. Besides the oscillations in figure 15 are due to the variations of these parameters.

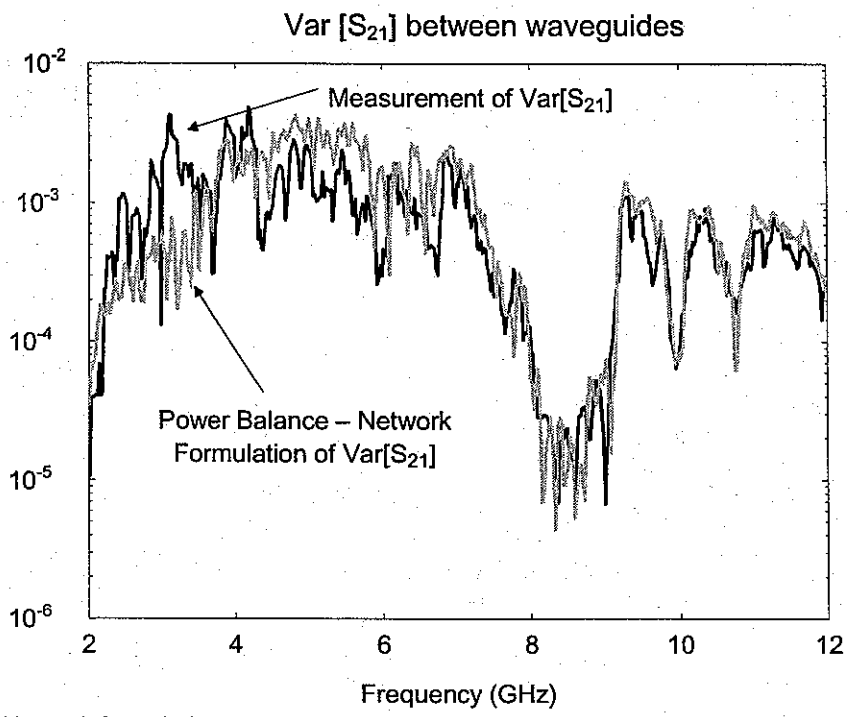

Figure 15 : Network formulation of the power balance approach applied to the test case – Measurement and computation (via Network Formulation) of Var[S_{21}]

6. CONCLUSION

In this work, we have shown the capability of the power balance approach to estimate high frequency coupling mechanisms. Furthermore, we proved how easy it is to implement this technique by using a network formulation. The great interests of this technique are its rapidity of computation, and because it does not require an accurate description of the system geometry and finally because it is only based on analytical formulas.

Nevertheless, fundamental research are essential to :

- evaluate the limits of application of this technique, for example the lower and upper frequency limits compared to the systems dimensions. Further experimentation must be performed in order to analyze if we can still consider that an equipment filled with electronic cards behaves as a pseudo-mode stirring chamber.
- take into account the coupling of the internal electromagnetic environment with bundles and cables, and investigate how this coupling must be introduced in the network formulation,
- obtain a complete data bank of coupling cross sections of POEs. So far, we only have analytical expressions for generic apertures. We must also analyze specific cases, such as cables running through apertures.

Those different topics will be investigated in the future. From the point of view of CRIPTE development, the work should therefore focus on :

- validations with more complex configurations,
- improved models for tubes and junctions,
- the reduction of the actual CRIPTE version (transmission line oriented version) to a more specific Power Balance oriented version.
- introduction of original Electromagnetic Topology formalism in the network approach.

The efficiency of this technique and the encouraging results we obtained on this simple geometry example must not make us forget that the approach is based on statistics and probability. Therefore, its application depends on the type of objective aimed when solving the electromagnetic problem. For example, this method can not be directly applied for system vulnerability since we can not compute the worst case from a deterministic point of view. However, it is not obvious that there is a clear and commonly accepted definition of the 'worst case' in the scientific community.

Nevertheless, this promising approach will be very interesting for analyzing high frequency coupling in complex systems especially as long as no deterministic method is currently available to perform such an analysis.

7. REFERENCES

[1] D.A Hill & Co : Aperture excitation of electrically large lossy cavities - I.E.E.E Transactions on Electromagnetic Compatibility – August 1994

[2] C.D Taylor & C.W. Harrison : On the coupling of microwave radiation to wires structures – I.E.E.E Transactions on Electromagnetic Compatibility – August 1992

[3] A. Louis & C.L. Gardner : Bounds on aperture coupling from radar and other pulses - I.E.E.E Transactions on Electromagnetic Compatibility – November 1995

[4] K. Lee & F.C. Yang : Trends and bounds in RF coupling to a wire inside a slotted cavity – I.E.E.E Transactions on Electromagnetic Compatibility – August 1992

[5] W.J Karzas : Back door coupling of RF energy to spacecraft interior cabling – Interactions Notes 513 – February 1994

[6] T.A. Loughry : Frequency stirring : an alternate approach to mechanical mode stirring for the conduct of electromagnetic susceptibility testing – Philips Laboratory – November 1991

[7] H. Zaglauer : Coupling through composite fuselage – application of the Power Balance method – comparison with measurements and estimation of the efficiency of absorbing material within the cabin – CATE-DO-REP-003 – August 1999

[8] D.A Hill : A reflection coeffcient derivation for the Q of a reverberation chamber - I.E.E.E Transactions on Electromagnetic Compatibility – November 1996

[9] R. Holland & R. St John : Statistical responses of EM driven cables inside an overmoded enclosure - I.E.E.E Transactions on Electromagnetic Compatibility – November 1998

[10] R.E. Richardson : Mode stirred chamber calibration factor, relaxation time and scaling laws - I.E.E.E Transactions on Electromagnetic Compatibility – December 1985

[11] R. St John, J. Prewitt & R. Holland : How to think about electromagnetic interaction : a statistical approach – Interactions notes 559 – July 2000

[12] M.P. Robinson & Co : Analytical formulation for the shielding effectiveness of enclosures with apertures - I.E.E.E Transactions on Electromagnetic Compatibility – August 1998

[13] J.M. Dunn : Local high frequency analysis of the fields in a mode stirred chamber - I.E.E.E Transactions on Electromagnetic Compatibility – February 1999

[14] C.L. Gardner & P.A. Hrubik : An experimental and analytical study of the use of bounds to estimate the coupling to a monopole inside a cavity with an aperture – I.E.E.E Transactions on

Electromagnetic Compatibility – February 1999

[15] D.A. Hill : Plane wave integral representation for fields in reverberation chambers - I.E.E.E Transactions on Electromagnetic Compatibility – August 1998

[16] I. Junqua & F. Issac : Estimation du couplage électromagnétique haute fréquence dans une structure à plusieurs cavités par l'approche dite 'Power Balance' – Rapport ONERA RF 2/05594 DEMR – Janvier 2002, In French

[17] C.E. Baum : The Theory of Electromagnetic Interference Control, Modern Radio Science 1990, Oxford University Press, pp. 87-101. Also in Interaction Notes, Note 478, December 1989.

[18] C.E. Baum, T.K. Liu, F.M. Tesche : On the Analysis of General Multiconductor Transmission - Line Networks, Interaction Notes, Note 350;1978. Also inclued in C.E. Baum : Electromagnetic Topology for the Analysis and Design of Complex Systems, pp. 467-547 in J.E. Thompson and L. H. Heussen (eds.), "Fast Electrical and Optical Measurements", Martinus Nijhoff, Dordrecht, 1986.

[19] J.P. Parmantier, V. Gobin, F. Issac, L. Paletta, I. Junqua, Y. Daudy & J.M. Lagarde : ETEIII – Application of Electromagnetic Topology on the EMPTAC Aircraft, AFRL Interaction Notes, Note 527, May 1997